TOWARDS MICRO ELECTRICAL IMPEDANCE TOMOGRAPHY ON CHIP

D. Metz[1,2], B. Matheis[1], I. Constantinou[1,2]

[1] Technische Universität Braunschweig, Institute for Microtechnology; 38124; Braunschweig, Germany; d.metz@tu-braunschweig.de

[2] Technische Universität Braunschweig, Zentrum für Pharmaverfahrenstechnik (PVZ); 38106; Braunschweig, Germany

ABSTRACT

This work presents initial design and testing of a miniaturized electrical impedance tomography platform. Electrical impedance tomography (EIT) provides a low-cost, non-invasive, radiation-free type of imaging and can be relatively easily implemented on other miniaturized systems like microfluidics. Herein, we describe a miniaturized EIT on chip, along with its measurement setup and image reconstruction pipeline. First imaging results demonstrating a well-functioning setup are presented and form the basis for further investigations.

Keywords: Electrical Impedance Tomography

INTRODUCTION

Electrical impedance tomography (EIT) is a low-cost, non-invasive, and radiation-free type of medical imaging [1–3]. EIT relies on the estimation of the conductivity of an object, based on currents/voltages applied to its surface. A typical medical application of EIT is the study of respiratory patterns. In this case, electrodes are placed on a transverse plane around the patient's chest. During breathing, the volume of the lungs changes. This change can be measured as a change in conductivity, since air and lung tissue have different conductivities [4]. In this project, we aim to miniaturize EIT for future applications in the characterization of biological samples on other miniaturized platforms such as organ-on-chip. Previous work already demonstrates the utility of EIT for detection/monitoring of biological samples and provides some proof of concept [5, 6]. The cost of integrating and fabricating electrodes in such microsystems remains low compared to the extensive and fast imaging results that can be achieved. However, progress still needs to be made on the reconstruction side, since low resolution remains a limitation.

Herein, we report on the development of a simplified EIT-on-chip platform and first imaging results using the implemented measurement setup. A brief introduction to the principles of EIT measurement and theory of image reconstruction is followed by a detailed description of the chip, its design, and the measurement setup. Finally, a first EIT-imaging experiment is presented and discussed.

RESEARCH CONCEPT

EIT measurement principle

During EIT measurements, samples are placed within an electrode array positioned on the inner surface of an imaging chamber. Then N small alternating currents $i_{i,j}$ are injected between electrode pairs i and j. After a short delay intended to allow the electric field to build up inside the cell culture chamber, a series of M voltage measurements are made between electrode pairs ($U_{i,j}$) for each injection. A complete measurement set of $N \times M$ voltages is obtained and used for the reconstruction of impedance maps. Different electrode arrangements, injection and measurement patterns can be used. A commonly used ring arrangement of 16 electrodes, as shown in Figure 1, is usually employed in combination with the “adjacent” injection and measurement pattern. Currents and voltages are injected and measured between each neighboring electrode ($j = i + 1$). In this case, the measurement set is composed of 16 injections x 16 measurements = 256 voltage measurements.

https://doi.org/10.24355/dbbs.084-202110251619-0

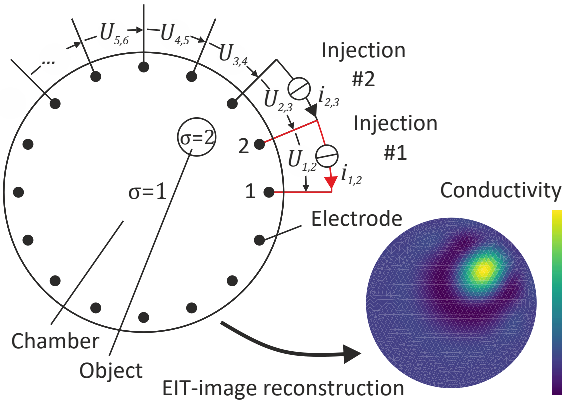

Figure 1: Principle of EIT measurement in a chamber with 16 electrodes arranged in a ring configuration. Adjacent injection and measurement pattern is partially shown.

EIT image reconstruction

In EIT, the conductivity $\boldsymbol{\sigma}$ of a body can be related to the measured voltages $\boldsymbol{U}$ through a non-linear function, F, also known as the forward model, as:

$$\boldsymbol{U} = F(\boldsymbol{\sigma}) \tag{1}$$

In practice, this relation is linearized and reduced to a Jacobian matrix $\boldsymbol{J}$ as given in Eq. (2). This matrix describes the sensitivity of the electrode array for the given injection and measurement pattern. For more detailed definitions, see the works in [4, 7].

$$\boldsymbol{U} = \boldsymbol{J} \cdot \boldsymbol{\sigma} \tag{2}$$

EIT image reconstruction is achieved by solving the inverse problem, where $\boldsymbol{U}$ is known and $\boldsymbol{\sigma}$ is searched. Usually this is done using standard regularization methods such as the one-step Gauss-Newton method [8]. In this work, the open-source Python package pyEIT has been used for image reconstruction [3]. Less developed than the popular open-source Matlab toolbox EIDORS [9], pyEIT allows rapid prototyping of EIT systems and is easily extensible. In pyEIT, a 2D chamber can be modeled as a finite element model using a reimplemented "distmesh" generator in Python. Typical dynamic EIT image reconstruction techniques are implemented and can be easily used.

This work focused on time-difference imaging (see also frequency-difference in [6]) using the dynamic Jacobian matrix reconstruction method implemented in the pyEIT package, similar to the one-step Gauss-Newton method. For EIT imaging, the voltage differences $\Delta\boldsymbol{U} = \boldsymbol{U_t} - \boldsymbol{U_0}$ need to be formed from the current measured voltages $\boldsymbol{U_t}$ and the initial voltages $\boldsymbol{U_0}$ (reference), and used to calculate the normalized conductivity changes $\Delta\boldsymbol{\sigma}$ as follows:

$$\Delta\boldsymbol{\sigma} = -((\boldsymbol{J}^T\boldsymbol{J} + \lambda\boldsymbol{R})^{-1} \cdot \boldsymbol{J}^T) \cdot \Delta\boldsymbol{U_{nom}} \tag{3}$$

where λ is the regularization hyperparameter, $\boldsymbol{R}$ is the regularization matrix as: $\boldsymbol{R}_{i,i} = [\boldsymbol{J}^T\boldsymbol{J}]_{i,i}{}^p$ and $\Delta\boldsymbol{U_{nom}} = \frac{\Delta\boldsymbol{U}}{|\boldsymbol{U_0}|}$ are the normalized voltage differences. Here $\lambda = 0.01$, and $p = 0.5$ were used.

Chip platform

The ultimate goal of the project is to build an organ-on-chip platform similar to the one shown in Figure 2a, capable of monitoring the growth or behavior of cells (or other biological samples) placed/cultured in the center of the chamber, e.g., on a membrane. For EIT measurements within the chamber volume, electrode arrays should be integrated at the bottom and top of the chamber. As a first step, a simpler platform was developed and investigated, with an electrode array integrated on only one side of the chamber (Figure 2b). The platform consists of a 10 × 20 mm microfabricated chip (Figure 2c) placed in a 3D-printed holder to obtain an imaging chamber with a diameter of 5 mm and a height of 2 mm.

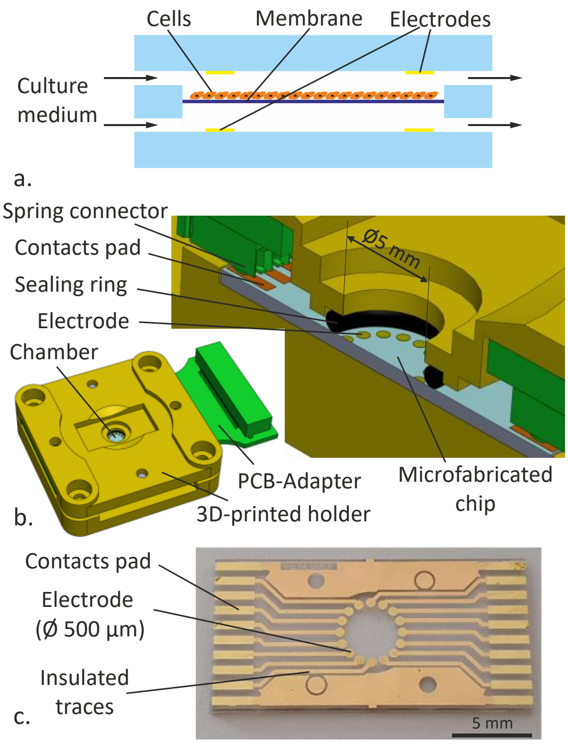

Figure 2: a. Schematic of planned organ-on-chip with electrode arrays on top and bottom of cell culture chamber, b. chip used in this work, electrode arrays only on one side, c. microfabricated chip used in b.

Electrodes of sputtered gold (about 400 nm thickness) were fabricated on the chip made of glass and structured by photolithographic wet etching. Finally, the electrical traces were insulated using a PECVD silicon oxide (SiO2) layer (about 300 nm thickness). Contact pads were placed at the ends of the chip for fast and easy electrical contacting of the electrodes. These contact

https://doi.org/10.24355/dbbs.084-202110251619-0

pads match the spring connectors of the PCB adapter for the EIT measuring device (Figure 3).

EIT measurement setup

An EIT device from Sciospec GmbH [10] was used for the EIT measurements (Figure 3). The device can deliver injection currents from 10 mA down to 100 nA with a frequency range of 100 Hz – 100 kHz and measure the voltages of up to 32 channels simultaneously. Voltages are measured using lock-in amplifier electronics in combination with a special "SineFit" algorithm from Sciospec. The connection to the OoC is made via a high-speed coaxial cable from Samtec (FCF8, see also connector FCS8).

A custom graphical user interface (GUI) was implemented in Python using pyQt5 to set up the device, capture and store the measurement voltages. The corresponding top view of the chamber was captured using a micro-camera. Thanks to multiprocessing implementation, this GUI allows live viewing of the measurement data and EIT imaging with pyEIT at a rate of up to 1 frame/s.

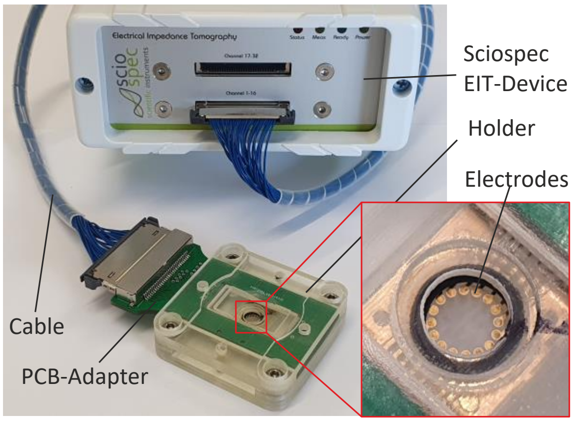

Figure 3: Micro-EIT platform connected to the Sciospec EIT measurement device.

RESULTS

To validate the measurement setup, the chamber was filled with Danieau's solution (conductive liquid) [11]. After measuring the reference/initial voltage $\boldsymbol{U_0}$, an object (Ø1 × 0.4 mm) made of an insulator (EPDM) was inserted into the chamber at two different positions. For both positions, the voltages $\boldsymbol{U_{ti}}$ were measured and an EIT image was calculated using the difference with $\boldsymbol{U_0}$. Measurements were performed with an injection current of 10 µA at a frequency of 10 kHz and adjacent injection and measurement patterns.

Figure 4 shows both experiments, the 256 measured voltages differences $\Delta\boldsymbol{U}$, the EIT reconstructed image, and a top view image of the chamber for comparison. The reconstructed impedance map shows normalized conductivity difference in comparison with the chamber without object. Each 16 measurements correspond to one injection pattern. In Figure 4a, we can observe that the highest voltage difference happens around injection #14 ($i_{14,15}$), which coincides with the position of the object. The position of the object, based on the chamber-top-view, was added to the reconstructed image as a circle to appreciate the reconstruction quality.

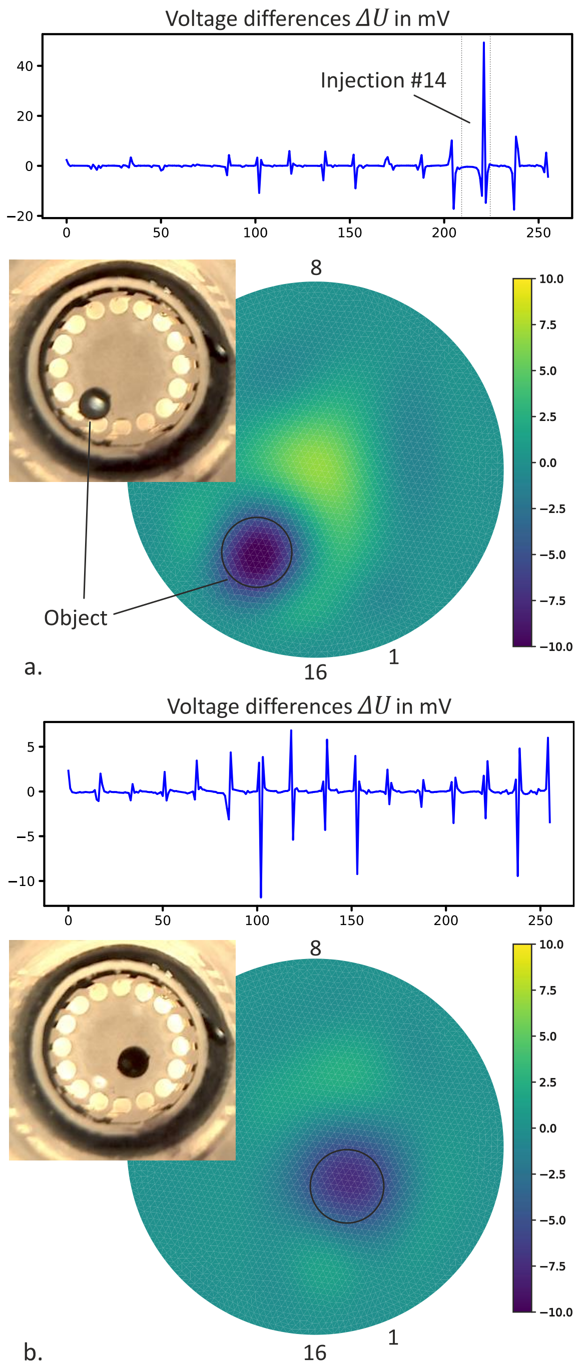

Figure 4: EIT imaging results with objet at different positions.

https://doi.org/10.24355/dbbs.084-202110251619-0

DISCUSSION

In Figure 4, same conductivity changes can be observed for the same object in the same liquid but at a different positions. Also, the position of the object in the EIT image matches its actual position in the chamber. This attests to a successful EIT imaging, validating the developed setup. A better contrast between the object and the medium can be observed in Figure 4a than in Figure 4b. This is related to the high sensitivity of the ring electrode arrangement with adjacent patterning and an object closer to the electrodes, as shown in [3]. However, this also leads to more artefacts, as observed in Figure 4a.

CONCLUSIONS

In this work, a first version of a miniaturized EIT has been presented and first investigations show the good functionality of the measurement setup and image reconstruction implemented on Python using the pyEIT package.

In the future, further investigations will be performed specifically for the imaging of biological samples. Additionally, modeling in pyEIT should be extended for better modeling in 2D and 3D (e.g. with planar electrodes). The use of machine learning should also be explored to improve image resolution and quality of the reconstruction [7]. In the future, a closed chip design will be considered for constant volume during long-term experiments.

ACKNOWLEDGMENT

This work has been performed within the framework of the SMART BIOTECS alliance between the Technische Universität Braunschweig and the Leibniz Universität Hannover. This initiative is supported by the Ministry of Science and Culture (MWK) of Lower Saxony, Germany.

REFERENCES

[1] A. Adler and A. Boyle, “Electrical Impedance Tomography: Tissue Properties to Image Measures,” *IEEE transactions on bio-medical engineering*, vol. 64, no. 11, pp. 2494–2504, 2017, doi: 10.1109/TBME.2017.2728323.

[2] D. S. Holder, Ed., *Electrical impedance tomography: Methods, history and applications*. Bristol: Institute of Physics, 2005. [Online]. Available: http://www.loc.gov/catdir/enhancements/fy0653/2005279767-d.html

[3] B. Liu *et al.,* “pyEIT: A python based framework for Electrical Impedance Tomography,” *SoftwareX*, vol. 7, pp. 304–308, 2018, doi: 10.1016/j.softx.2018.09.005.

[4] A. Adler and A. Boyle, “Electrical Impedance Tomography,” in *Wiley Encyclopedia of Electrical and Electronics Engineering*, J. G. Webster, Ed.: Wiley, 1999, pp. 1–16.

[5] Y. Yang, J. Jia, S. Smith, N. Jamil, W. Gamal, and P.-O. Bagnaninchi, “A Miniature Electrical Impedance Tomography Sensor and 3-D Image Reconstruction for Cell Imaging,” *IEEE Sensors J.*, vol. 17, no. 2, pp. 514–523, 2017, doi: 10.1109/JSEN.2016.2631263.

[6] Y. Yang and J. Jia, “A multi-frequency electrical impedance tomography system for real-time 2D and 3D imaging,” *The Review of scientific instruments*, vol. 88, no. 8, p. 85110, 2017, doi: 10.1063/1.4999359.

[7] M. Schwarz, M. Jendrusch, and I. Constantinou, “Spatially resolved electrical impedance methods for cell and particle characterization,” *Electrophoresis*, vol. 41, 1-2, pp. 65–80, 2020, doi: 10.1002/elps.201900286.

[8] A. Adler, T. Dai, and W. R. B. Lionheart, “Temporal image reconstruction in electrical impedance tomography,” *Physiol. Meas.*, vol. 28, no. 7, S1-11, 2007, doi: 10.1088/0967-3334/28/7/S01.

[9] A. Adler and W. R. B. Lionheart, “Uses and abuses of EIDORS: an extensible software base for EIT,” *Physiol. Meas.*, vol. 27, no. 5, S25-42, 2006, doi: 10.1088/0967-3334/27/5/S03.

[10] Sciospec, *Discover Sciospec's powerful EIT platform - Sciospec.* [Online]. Available: https://www.sciospec.com/eit/ (accessed: Jul. 20 2021).

[11] “Danieau's Solution,” *Cold Spring Harbor Protocols*, vol. 2013, no. 5, pdb.rec074260-pdb.rec074260, 2013, doi: 10.1101/pdb.rec074260.

https://doi.org/10.24355/dbbs.084-202110251619-0